

JYX



This is a self-archived version of an original article. This version may differ from the original in pagination and typographic details.

Author(s): ALICE Collaboration

Title: Measurement of Prompt D^0 , Λ_c^+ , and $\Sigma_c^{0,++}(2455)$ Production in Proton-Proton Collisions at $\sqrt{s} = 13$ TeV

Year: 2022

Version: Published version

Copyright: © 2022 CERN, for the ALICE Collaboration

Rights: CC BY 4.0


Rights url: <https://creativecommons.org/licenses/by/4.0/>

Please cite the original version:

ALICE Collaboration. (2022). Measurement of Prompt D^0 , Λ_c^+ , and $\Sigma_c^{0,++}(2455)$ Production in Proton-Proton Collisions at $\sqrt{s} = 13$ TeV. *Physical Review Letters*, 128(1), Article 012001. <https://doi.org/10.1103/PhysRevLett.128.012001>

Measurement of Prompt D^0 , Λ_c^+ , and $\Sigma_c^{0,++}$ (2455) Production in Proton-Proton Collisions at $\sqrt{s} = 13$ TeV

S. Acharya *et al.**
(ALICE Collaboration)

 (Received 25 August 2021; revised 9 November 2021; accepted 24 November 2021; published 5 January 2022)

The p_T -differential production cross sections of prompt D^0 , Λ_c^+ , and $\Sigma_c^{0,++}$ (2455) charmed hadrons are measured at midrapidity ($|y| < 0.5$) in pp collisions at $\sqrt{s} = 13$ TeV. This is the first measurement of $\Sigma_c^{0,++}$ production in hadronic collisions. Assuming the same production yield for the three $\Sigma_c^{0,++}$ isospin states, the baryon-to-meson cross section ratios $\Sigma_c^{0,++}/D^0$ and Λ_c^+/D^0 are calculated in the transverse momentum (p_T) intervals $2 < p_T < 12$ and $1 < p_T < 24$ GeV/ c . Values significantly larger than in e^+e^- collisions are observed, indicating for the first time that baryon enhancement in hadronic collisions also extends to the Σ_c . The feed-down contribution to Λ_c^+ production from $\Sigma_c^{0,++}$ is also reported and is found to be larger than in e^+e^- collisions. The data are compared with predictions from event generators and other phenomenological models, providing a sensitive test of the different charm-hadronization mechanisms implemented in the models.

DOI: [10.1103/PhysRevLett.128.012001](https://doi.org/10.1103/PhysRevLett.128.012001)

The formation of hadrons out of quarks (“hadronization”) represents a fundamental process in nature that can be investigated at particle colliders where, at high collision energies, quarks represent the relevant degrees of freedom for a very short time on the order of 10^{-23} s. The measurement of the relative production rates of different charm-hadron species allows us to study how charm quarks, produced only in initial hard scatterings, combine with other quarks, which may either exist in the system before hadronization or be produced in the strong-force potential at hadronization time. Recent measurements of Λ_c^+ , Ξ_c^0 , and Λ_b^0 -baryon production in pp collisions at $\sqrt{s} = 5.02, 7,$ and 13 TeV [1–8] indicate that the production of charm and beauty baryons relative to that of charm and beauty mesons is enhanced in pp with respect to e^+e^- and ep collisions [9–15]. Several models tuned to reproduce the e^+e^- data significantly underestimate the ratios measured in pp collisions and do not describe the observed transverse-momentum (p_T) trends. These measurements also set kinematic boundaries to the validity of the assumption made in perturbative-QCD calculations like fixed order next to leading log (FONLL) [16,17] and general mass-variable flavour number scheme (GM-

VFNS) [18–23] that fragmentation functions tuned on e^+e^- and ep data can be used in pp collisions.

The $\Sigma_c^{0,++}$ baryon triplet is the isospin $I = 1$ partner of the singlet ($I = 0$) Λ_c^+ baryon. All these states are composed of a charm quark and a pair of light (u, d) quarks. In e^+e^- collisions, while in the light-flavor sector the mass dependence of the yields of the Σ and Λ states is well described by a single exponential function, the yields of the $\Sigma_c^{0,++}$ states are about a factor 4 smaller than those of the Λ_c^+ states [24]. In the framework of hadronization via string fragmentation, this suppression can be ascribed to the need to form $\Sigma_c^{0,++}$ via the combination of a heavy charm quark, which is always a string end point, and a diquark with spin $S = 1$ and $I = 1$ formed via the Schwinger tunneling process [24,25]. The large mass of $S = 1$ diquarks suppresses their formation with respect to $S = 0$ diquarks, hence the $\Sigma_c^{0,++}$ production yield is suppressed with respect to the Λ_c^+ yield. In the models that provide a fair description of the Λ_c^+/D^0 ratio in pp collisions (here denoted as “CR-BLC” [25], “SHM + RQM” [26], “Catania” [27,28], and “QCM” [29]) this suppression mechanism is absent or heavily reduced, and a sizable contribution to Λ_c^+ production from strong decays of $\Sigma_c^{0,++}$ states is expected. Therefore, the measurement of the ground-state $\Sigma_c^{0,++}$ (2455) production is fundamental to understand the dynamics of heavy-flavor baryon formation, providing a key test for the different scenarios proposed in the mentioned models. Among these, the CR-BLC model is a version of PYTHIA8 in which terms beyond the leading-color approximation (BLC) are considered in string formation, representing more accurately the QCD SU

*Full author list given at the end of the article.

Published by the American Physical Society under the terms of the [Creative Commons Attribution 4.0 International license](https://creativecommons.org/licenses/by/4.0/). Further distribution of this work must maintain attribution to the author(s) and the published article’s title, journal citation, and DOI. Funded by SCOAP³.

(3) algebra and de facto enhancing effects from color reconnection (CR). These terms cause confining potentials to also arise between quarks not produced in the same hard scattering and are relevant to hadronic collisions at high energies, where multiple-parton interactions produce an environment rich in quarks and gluons. Moreover, they give rise to “junction topologies” that favor the production of baryon states and do not penalize the formation of $\Sigma_c^{0,+,++}$ with respect to Λ_c^+ states. The production of $\Sigma_c^{0,+,++}$ (2455) is expected to increase by large factors, up to 25, and become even larger than that of direct Λ_c^+ . The SHM + RQM model predicts a large feed-down contribution to the Λ_c^+ ground state from an enriched set of mostly unobserved excited charm-hadron states expected from the relativistic quark model (RQM [30]). The branching fractions of charm quarks to the various hadron species are assumed to follow the relative thermal densities calculated with the statistical hadronization model (SHM [31]), therefore to depend only on the state mass and spin-degeneracy factor. In the Catania model, charm quarks can hadronize via “vacuumlike” fragmentation as well as recombine (coalesce) with surrounding light quarks from the underlying event. The Wigner formalism is used to calculate the probability to form a baryon (meson) given the phase-space distribution of three (two) quarks. A different formalism is implemented in the “quark (re)combination mechanism” (QCM) model, in which charm quarks form hadrons by combining with equal-velocity light quarks. In this model, the relative abundances of the different baryon species are fixed by thermal weights.

In this Letter, the measurement performed with the ALICE experiment of the p_T -differential cross sections of prompt D^0 , Λ_c^+ , and $\Sigma_c^{0,+,++}$ (2455) in pp collisions at $\sqrt{s} = 13$ TeV at midrapidity ($|y| < 0.5$) is reported. This is the first production measurement for $\Sigma_c^{0,+,++}$ (2455) in hadronic collisions. The baryon-to-meson ratios Λ_c^+/D^0 and $\Sigma_c^{0,+,++}/D^0$ as well as the fraction of Λ_c^+ feed-down from $\Sigma_c^{0,+,++}$ decays ($\Lambda_c^+ \leftarrow \Sigma_c^{0,+,++}/\Lambda_c^+$) are compared with expectations from the theoretical models described above. These ratios are calculated assuming the three $\Sigma_c^{0,+,++}$ (2455) isospin states to be equally produced. In what follows, the symbols $\Sigma_c^{0,++}$ and $\Sigma_c^{0,+,++}$ always refer to the ground-state $\Sigma_c^{0,+,++}$ (2455) baryons.

The ALICE apparatus is described in detail in Refs. [32,33]. The D^0 , Λ_c^+ , and $\Sigma_c^{0,++}$ decays are reconstructed in the central barrel, which covers the pseudorapidity interval $|\eta| < 0.9$ and is embedded in a cylindrical solenoid providing a magnetic field of 0.5 T parallel to the beam direction. Charged particles are tracked with the inner tracking system (ITS) and the time projection chamber (TPC). The ITS detector consists of six cylindrical silicon layers surrounding the beam pipe. The measurement of the specific energy loss (dE/dx) in the TPC gas and of the time difference between the collision time and the particle arrival

time at the time-of-flight (TOF) detector are exploited for particle identification (PID) [1,34].

The data were collected with a minimum bias trigger requiring coincident signals in the two scintillator arrays covering the intervals $2.8 < \eta < 5.1$ (V0A) and $-3.7 < \eta < -1.7$ (V0C). Only events with a primary vertex reconstructed within ± 10 cm from the nominal interaction point along the beam line were analyzed. Events with multiple primary vertices were rejected in order to remove collision pileup in the same bunch crossing. The remaining undetected pileup is negligible. The selected events correspond to an integrated luminosity of $\mathcal{L}_{\text{int}} = 31.9 \pm 0.5 \text{ nb}^{-1}$ [35].

The following hadronic decay channels are reconstructed to measure the production of the $\Sigma_c^{0,++}$, Λ_c^+ , and D^0 particles and their antiparticles. The $\Sigma_c^{0,++}$ baryons decay strongly to a Λ_c^+ in the channel $\Sigma_c^{0,++} \rightarrow \pi^- \Lambda_c^+$ with a branching ratio (BR) of about 100% [36]. The Λ_c^+ baryons are reconstructed in two different final states: $\Lambda_c^+ \rightarrow pK^-\pi^+$, which occurs via multiple resonant and nonresonant decay channels, with a total BR of $(6.28 \pm 0.32)\%$ and $\Lambda_c^+ \rightarrow pK_S^0$, with a BR of $(1.59 \pm 0.08)\%$, followed by $K_S^0 \rightarrow \pi^+\pi^-$ with a BR of $(69.20 \pm 0.05)\%$. The D^0 mesons are reconstructed in the $D^0 \rightarrow K^-\pi^+$ decay channel, which has a BR of $(3.95 \pm 0.03)\%$.

The measurements of the D^0 and Λ_c^+ cross sections are based on an invariant-mass analysis of signal candidates selected for having the proper daughter-particle identities and a displaced decay topology. The analysis procedure, described only briefly here, closely follows that of previous measurements [1,4,37]. The D^0 candidates are formed by combining pairs of tracks with opposite charge, each with $|\eta| < 0.8$, $p_T > 0.3$ GeV/ c , and selected according to the track-quality criteria described in Ref. [37], which are adopted also in the Λ_c^+ and $\Sigma_c^{0,++}$ analyses. Pions and kaons are identified by requiring the dE/dx and time-of-flight measured, respectively, with the TPC and TOF to be within 3 times the detector resolution from the expected values. The topological selections applied to reduce the combinatorial background are the same as those reported in Ref. [37]. For the $\Lambda_c^+ \rightarrow pK^-\pi^+$ decay channel, Λ_c^+ candidates are formed by combining tracks identified as p , K , or π , using the Bayesian PID approach with the “maximum-probability criterion” [38]. The reconstruction of the $\Lambda_c^+ \rightarrow pK_S^0$ decay is based on a machine-learning classification that makes use of the boosted decision trees algorithm [39]. For both decay channels, a complete description of the applied PID and topological selections can be found in Ref. [1]. A fiducial-acceptance selection $|y| < y_{\text{fid}}(p_T)$ is applied to the D^0 and Λ_c^+ candidates, with y_{fid} smoothly increasing from about 0.6 at $p_T = 1$ GeV/ c to the maximum value of 0.8 at $p_T = 5$ GeV/ c .

For the $\Sigma_c^{0,++}$ study, separate analyses are carried out with candidates obtained from the two Λ_c^+ decay channels:

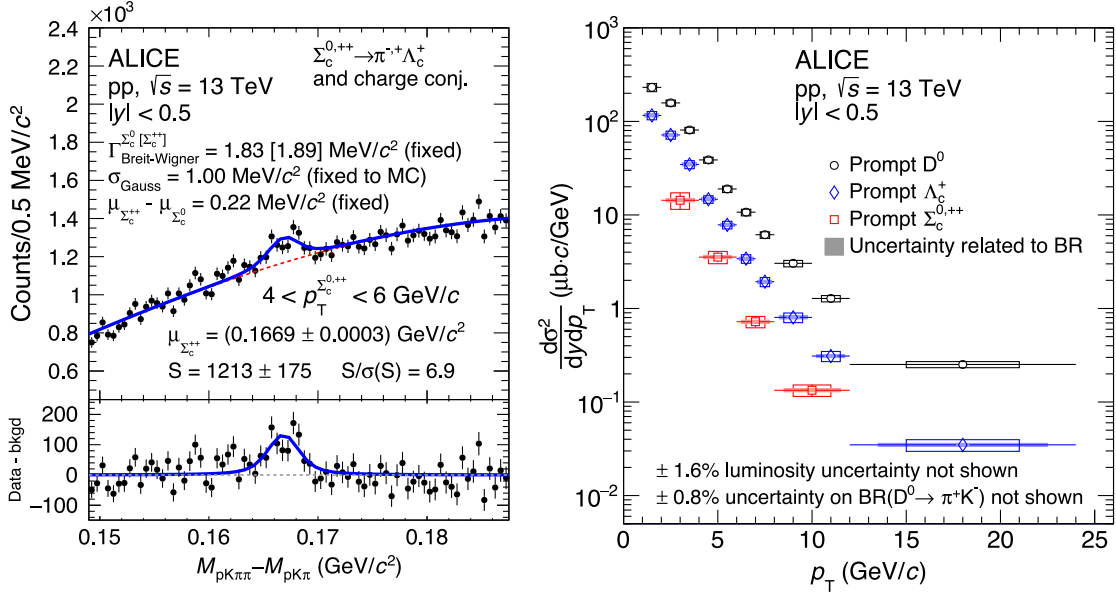


FIG. 1. Left: distribution of $\pi^+ K^- p \pi^\pm$ to $\pi^+ K^- p$ (and charge conjugate) invariant-mass difference in $4 < p_T^{\Sigma_c^{0,++}} < 6$ GeV/c. Right: p_T -differential cross section of prompt D^0 , Λ_c^+ , and $\Sigma_c^{0,++}$ in pp collisions at $\sqrt{s} = 13$ TeV. The statistical and systematic uncertainties are shown as vertical lines and boxes, respectively.

averages are then taken of the resulting cross sections and particle cross section ratios. For the study of the $\Lambda_c^+ \leftarrow \Sigma_c^{0,++}$ feed-down, the analysis is performed as a function of $\Lambda_c^+ p_T$, rather than $\Sigma_c^{0,++} p_T$. The $\Sigma_c^{0,++}$ candidates are built by pairing Λ_c^+ candidates with invariant mass in the interval $2.26 \lesssim M(\Lambda_c^+) \lesssim 2.31$ GeV/c² with charged particles with $|\eta| < 0.9$ and $p_T > 0.12$ GeV/c. The decay tracks are further selected for having a distance from the primary vertex smaller than 650 μm in the transverse plane ($d_{r\phi}$) and 1.5 mm along the beam axis. The signal-to-background ratio for the $\Sigma_c^{0,++}$ reconstructed with $\Lambda_c^+ \rightarrow pK^- \pi^+$ candidates is improved by requiring $|d_{r\phi} - d_{r\phi}^{\text{expected}}|/\sigma(d_{r\phi}) < 2.5$ for $4 < p_T < 6$ GeV/c [40] and $\cos \theta_{\text{point}} > 0.8$ for $2 < p_T < 6$ GeV/c, where θ_{point} is the angle between the Λ_c^+ flight line and its reconstructed momentum vector.

The $\Sigma_c^{0,++}$ and $\Lambda_c^+ \leftarrow \Sigma_c^{0,++}$ raw yields are estimated in each p_T interval via a binned-likelihood fit to the distribution of the $\Sigma_c^{0,++}$ and Λ_c^+ candidate invariant-mass difference ΔM . An example of a ΔM distribution is shown in Fig. 1 (left) for the $\Lambda_c^+ \rightarrow pK^- \pi^+$ decay channel for $4 < p_T^{\Sigma_c^{0,++}} < 6$ GeV/c. The function used to fit the signal peak is

$$f(\Delta M) = \frac{C}{2} [\mathfrak{B}(\Delta M - \mu_{\Sigma_c^{0,++}}; \sigma, \Gamma_{\Sigma_c^{0,++}}) + \mathfrak{B}(\Delta M - \mu_{\Sigma_c^0} + \delta M; \sigma, \Gamma_{\Sigma_c^0})], \quad (1)$$

where \mathfrak{B} is a Voigt function defined as the convolution of a Gaussian function and a Breit-Wigner function. Two Voigt

functions are used to account for Σ_c^0 ($M = 2453.75 \pm 0.14$ MeV/c², full width $\Gamma_{\Sigma_c^0} = 1.83_{-0.19}^{+0.11}$ MeV/c²) and Σ_c^{++} ($M = 2453.97 \pm 0.14$ MeV/c², $\Gamma_{\Sigma_c^{++}} = 1.89_{-0.18}^{+0.09}$ MeV/c²) isospin partners, whose invariant masses differ by $\delta M = 0.22$ MeV/c² [36]. The standard deviation of the Gaussian function, which accounts for the detector ΔM resolution, is fixed to values $\sigma \sim 1$ MeV/c², determined from Monte Carlo (MC) simulations. The free parameters of the fit are $\mu_{\Sigma_c^{0,++}}$, i.e., the $\Sigma_c^{0,++}$ peak mean, and C , which represents the sum of Σ_c^0 and Σ_c^{++} (and charge conjugates) raw yields. Depending on the p_T interval, the background ΔM distribution is described with a third-order polynomial function, a “threshold” function, or a template distribution, as described in the Supplemental Material [41]. The statistical uncertainty of the raw yields varies between 15% and 30% depending on the decay channel and p_T interval. It was verified that the Σ_c^0 and Σ_c^{++} raw yields are compatible within statistical uncertainties.

The p_T -differential cross sections of prompt D^0 , Λ_c^+ , $\Lambda_c^+ \leftarrow \Sigma_c^{0,++}$, and $\Sigma_c^{0,++}$ are calculated from the raw yields $N_{|y| < y_{\text{fid}}}$, measured in the fiducial y acceptance in a p_T interval of width Δp_T , as

$$\frac{d\sigma}{dp_T} \Big|_{|y| < 0.5} = \frac{1}{2} \frac{1}{\Delta p_T} \times \frac{f_{\text{prompt}} \times N_{|y| < y_{\text{fid}}}}{c_{\Delta y} \times (A \times \epsilon)_{\text{prompt}}} \times \frac{1}{\text{BR}} \times \frac{1}{\mathcal{L}_{\text{int}}}. \quad (2)$$

The factor 2 in the denominator takes into account that both particles and antiparticles contribute to the measured raw yields. The term $c_{\Delta y}$ encompasses the correction for the

rapidity coverage [40] and $(A \times \varepsilon)$ the detector acceptance, as well as the reconstruction and selection efficiency for the signal. This is estimated from Monte Carlo simulations in which pp collisions are simulated with the PYTHIA8.243 event generator [42,43] and the generated particles are propagated through the apparatus using the GEANT3 package [44] via a simulation that reproduces the detector layout and data-taking conditions. For prompt $\Sigma_c^{0,++}$, $c_{\Delta y} \times (A \times \varepsilon)$ increases from 1% (4%) in $2 < p_T < 4$ GeV/ c to 11% (22%) in $8 < p_T < 12$ GeV/ c in the $\Lambda_c^+ \rightarrow pK_S^0 \pi^+$ ($\Lambda_c^+ \rightarrow pK_S^0$) analysis.

The fraction of prompt particles contributing to the measured raw yield, f_{prompt} , is calculated using the reconstruction efficiencies of prompt and feed-down signals and the feed-down Λ_c^+ and D^0 cross sections, from Λ_b^0 and B meson decays (“beauty feed-down”). The latter cross sections are estimated as reported in Refs. [4,37], using computations based on FONLL calculations [16,17], beauty-quark fragmentation fractions determined from LHCb data [8] for $b \rightarrow \Lambda_b^0$, and from the averaged b -quark fragmentation fraction from the LEP [12] for $b \rightarrow B$, and modeling the $\Lambda_b^0 \rightarrow \Lambda_c^+ + X$ and $B \rightarrow D^0 + X$ decay kinematics with PYTHIA8 simulations [45]. The values of f_{prompt} range from 0.8 to 0.96 depending on p_T and the particle species. In the $\Sigma_c^{0,++}$ case, according to currently known decays [36] and to PYTHIA8 simulations, a non-negligible feed-down contribution is only expected from Λ_b^0 decays. The probability for $\Lambda_b^0 \rightarrow \Sigma_c^{0,++} + X$ decays is estimated to be about 3% of the probability for $\Lambda_b^0 \rightarrow \Lambda_c^+ + X$ decays, resulting in $f_{\text{prompt}} \geq 95\%$ for both $\Lambda_c^+ \leftarrow \Sigma_c^{0,++}$ and $\Sigma_c^{0,++}$ analyses.

Several sources of systematic uncertainties of the measured cross sections were studied, following similar procedures to those described in Refs. [4,37] for the Λ_c^+ and D^0 analyses. The uncertainty of $N_{|y| < y_{\text{fid}}}$, estimated by varying the invariant-mass fit procedure, ranges from 2% to 4% for D^0 and from 5% to 11% for Λ_c^+ , depending on p_T . For $\Sigma_c^{0,++}$ and $\Lambda_c^+ \leftarrow \Sigma_c^{0,++}$, this source provides the largest contribution to the systematic uncertainty, which was estimated by repeating the ΔM fits varying the signal and background fit functions, as well as the fit ranges. The Γ and δM parameters were varied within their uncertainties, and the Gaussian width σ was changed by $\pm 20\%$. The estimated uncertainty decreases from 15%–30% in the first p_T interval down to 8%–10% in the last one. Imperfections in the description of the apparatus and detector conditions in the Monte Carlo simulations introduce an uncertainty on the determination of the $c_{\Delta y} \times (A \times \varepsilon)_{\text{prompt}}$ correction factor: the systematic uncertainty of the track-reconstruction efficiency induces an uncertainty of about 4% for D^0 and 8% for Λ_c^+ and $\Sigma_c^{0,++}$, while the uncertainty related to the signal-selection efficiency, estimated by varying both topological and PID

selections, ranges between 3% and 10% depending on the p_T interval and particle species. Variations of the simulated signal spectrum p_T shapes based on FONLL (for D^0) and CR-BLC (for Λ_c^+ and $\Sigma_c^{0,++}$) models alter the efficiency by 2% for D^0 with $p_T < 2$ GeV/ c and, for the other analyses, by values decreasing from 10% to 1% with increasing p_T . The systematic uncertainty of the prompt fraction is about 2%–4% for D^0 and Λ_c^+ . For the $\Lambda_c^+ \leftarrow \Sigma_c^{0,++}$ and $\Sigma_c^{0,++}$ analyses, the beauty feed-down contribution was varied according to the Λ_c^+ feed-down uncertainty, with the additional variation from 3% to 6% of the ratio of $\Sigma_c^{0,++}$ and Λ_c^+ feed-down estimated with PYTHIA8 simulations as described previously. The resulting uncertainty of the cross section is within 2%. Further p_T -independent uncertainties derive from the BR and the luminosity. All the uncertainty sources described above are assumed to be uncorrelated with respect to each other. The total uncertainty in each p_T interval is calculated as the quadratic sum of the values estimated for each source.

The p_T -differential cross sections of D^0 , Λ_c^+ , and $\Sigma_c^{0,++}$ are shown in Fig. 1 (right). For Λ_c^+ and $\Sigma_c^{0,++}$, the weighted average of the results from the analyses of the two Λ_c^+ decay channels is calculated, using the inverse of the quadratic sum of the relative statistical and uncorrelated systematic uncertainties as weights. The total systematic uncertainty of the averaged Σ_c cross section varies from 20% at low p_T to 13% at high p_T . The cross section ratios Λ_c^+/D^0 and $\Sigma_c^{0,++}/D^0$ are compared with model expectations in Fig. 2 (left and middle panels). In the ratios, the systematic uncertainties of the track-reconstruction efficiency and luminosity, considered as fully correlated, cancel partly and completely, respectively. The feed-down uncertainty is propagated as partially correlated, while all other uncertainties are treated as uncorrelated. The Λ_c^+/D^0 ratio decreases with increasing p_T and is significantly larger than the ≈ 0.12 values observed in e^+e^- and ep collisions at several collision energies [12–15,46–48]. The values measured in pp collisions at $\sqrt{s} = 13$ TeV are compatible, within uncertainties, with those measured at $\sqrt{s} = 5.02$ TeV [3,4]. As shown in Fig. 2 (middle), the $\Sigma_c^{0,++}/D^0$ ratio is close to 0.2 for $2 < p_T < 6$ GeV/ c , and decreases with p_T down to about 0.1 for $8 < p_T < 12$ GeV/ c , though the uncertainties do not allow firm conclusions about the p_T dependence to be made. From Belle measurements (Table IV in Ref. [24]), the $\Sigma_c^{0,++}/\Lambda_c^+$ ratio in e^+e^- collisions at $\sqrt{s} = 10.52$ GeV can be evaluated to be around 0.17 and, thus, the $\Sigma_c^{0,++}/D^0$ ratio can be estimated to be around 0.02. Therefore, a remarkable difference is present between the pp and e^+e^- collision systems. Although rather approximate, such comparison is corroborated by the fact that a simulation performed with the default version of PYTHIA6.2 reasonably reproduces Belle data [24], while the default version of PYTHIA8.243 (Monash 2013 tune) severely

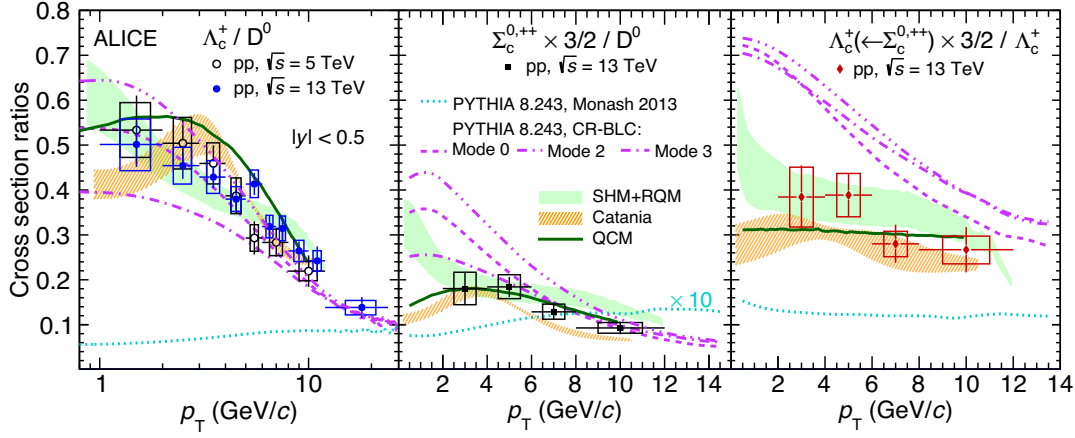


FIG. 2. Prompt-charm-hadron cross-section ratios: Λ_c^+/D^0 (left), $\Sigma_c^{0,+++}/D^0$ (middle), and $\Lambda_c^+ \leftarrow \Sigma_c^{0,+++}/\Lambda_c^+$ (right), in pp collisions at $\sqrt{s} = 13$ TeV, compared with model expectations [25–27,29] and (left) with data from pp collisions at $\sqrt{s} = 5.02$ TeV [3]. The horizontal lines reflect the width of the p_T intervals. The PYTHIA Monash 2013 curve is scaled by a factor of 10 in the middle panel.

underpredicts ALICE data, despite the very similar modeling of charm fragmentation in the two simulations. Figure 2 (right) shows the ratio $\Lambda_c^+ \leftarrow \Sigma_c^{0,+++}/\Lambda_c^+$ as a function of p_T , which quantifies the fraction of Λ_c^+ feed-down from $\Sigma_c^{0,+++}$. In order to better exploit the cancellation of correlated uncertainties, this is calculated as the weighted average of the ratios measured separately in the $\Lambda_c^+ \rightarrow pK^-\pi^+$ and $\Lambda_c^+ \rightarrow pK_S^0$ decay channels. The p_T -integrated value in the measured $p_T > 2$ GeV/ c interval is $0.38 \pm 0.06(\text{stat}) \pm 0.06(\text{syst})$, significantly larger than the ratio $\Sigma_c^{0,+++}/\Lambda_c^+ \sim 0.17$ from Belle data and the ~ 0.13 expectation from PYTHIA8 (Monash 2013) simulations. This indicates a larger increase for $\Sigma_c^{0,+++}/D^0$ than for the direct- Λ_c^+/D^0 ratio from e^+e^- to pp collisions. The larger feed-down from $\Sigma_c^{0,+++}$ partially explains the difference between the Λ_c^+/D^0 ratios in pp and e^+e^- collisions.

As shown in Figure 2, the CR-BLC (for which the three variations defined in Ref. [25] are considered), SHM + RQM, and Catania models describe, within uncertainties, both the Λ_c^+/D^0 and $\Sigma_c^{0,+++}/D^0$ ratios. The QCM model uses the Λ_c^+/D^0 data in pp collisions at $\sqrt{s} = 7$ TeV to set the total charm baryon-to-meson ratio, but it predicts correctly the $\Lambda_c^+ \leftarrow \Sigma_c^{0,+++}/\Lambda_c^+$ and the p_T shape of all ratios. The $\Lambda_c^+ \leftarrow \Sigma_c^{0,+++}/\Lambda_c^+$ ratio does not show a p_T trend as steep as that expected from the CR-BLC model, which significantly overestimates the Λ_c^+ feed-down from $\Sigma_c^{0,+++}$ at low p_T . Therefore, the data suggest that further tuning of the model parameters involving the reconnection of quarks via junction topologies is needed to possibly validate this as the mechanism reducing the assumed suppression of $\Sigma_c^{0,+++}$ formation in e^+e^- collisions [24,25]. In the Catania, QCM, and SHM + RQM models, no specific penalty factor affects the formation of Σ_c states. The fact that the SHM + RQM model reproduces both the

Λ_c^+/D^0 ratio and the fraction of Λ_c^+ feed-down from $\Sigma_c^{0,+++}$ may suggest that yet-unobserved higher-mass charm-baryon states exist and are formed more frequently in pp collisions than in e^+e^- and ep collisions. Similarly, the success of the Catania and QCM models in reproducing the data may indicate that charm hadronization in pp collisions involves coalescence of a charm quark with light quarks.

The p_T -differential cross section of $\Sigma_c^{0,+++}$ has been measured in pp collisions at $\sqrt{s} = 13$ TeV in the range $2 < p_T < 12$ GeV/ c , the first measurement in hadron-hadron collisions, together with the Λ_c^+ and D^0 cross sections in the range $1 < p_T < 24$ GeV/ c . The charm baryon-to-meson cross section ratios were found to be larger than expectations based on e^+e^- measurements. The reported results confirm previous observations at $\sqrt{s} = 5.02$ and $\sqrt{s} = 7$ TeV for the Λ_c^+ and show for the first time that the effect also extends to the $\Sigma_c^{0,+++}$. The feed-down from $\Sigma_c^{0,+++}$ decays to Λ_c^+ production amounts to $0.38 \pm 0.06(\text{stat}) \pm 0.06(\text{syst})$ in the range $2 < p_T < 12$ GeV/ c , which is significantly larger than measurements in e^+e^- collisions. The results presented provide important constraints on models aiming at explaining the observed increase of charm baryons in a parton-rich environment, either increasing baryon-formation probability via enhanced color reconnection or coalescence mechanisms, or assuming feed-down from yet-unobserved higher-mass baryon states.

The ALICE Collaboration would like to thank all its engineers and technicians for their invaluable contributions to the construction of the experiment and the CERN accelerator teams for the outstanding performance of the LHC complex. The ALICE Collaboration gratefully acknowledges the resources and support provided by all Grid centers and the Worldwide LHC Computing Grid

(WLCG) Collaboration. The ALICE Collaboration acknowledges the following funding agencies for their support in building and running the ALICE detector: A. I. Alikhanyan National Science Laboratory (Yerevan Physics Institute) Foundation (ANSI), State Committee of Science and World Federation of Scientists (WFS), Armenia; Austrian Academy of Sciences, Austrian Science Fund (FWF): [M 2467-N36], and National stiftung für Forschung, Technologie und Entwicklung, Austria; Ministry of Communications and High Technologies, National Nuclear Research Center, Azerbaijan; Conselho Nacional de Desenvolvimento Científico e Tecnológico (CNPq), Financiadora de Estudos e Projetos (Finep), Fundação de Amparo à Pesquisa do Estado de São Paulo (FAPESP), and Universidade Federal do Rio Grande do Sul (UFRGS), Brazil; Ministry of Education of China (MOEC), Ministry of Science and Technology of China (MSTC), and National Natural Science Foundation of China (NSFC), China; Ministry of Science and Education and Croatian Science Foundation, Croatia; Centro de Aplicaciones Tecnológicas y Desarrollo Nuclear (CEADEN), Cubaenergía, Cuba; Ministry of Education, Youth and Sports of the Czech Republic, Czech Republic; the Danish Council for Independent Research | Natural Sciences, the VILLUM FONDEN and Danish National Research Foundation (DNRF), Denmark; Helsinki Institute of Physics (HIP), Finland; Commissariat à l’Energie Atomique (CEA) and Institut National de Physique Nucléaire et de Physique des Particules (IN2P3) and Centre National de la Recherche Scientifique (CNRS), France; Bundesministerium für Bildung und Forschung (BMBF) and GSI Helmholtzzentrum für Schwerionenforschung GmbH, Germany; General Secretariat for Research and Technology, Ministry of Education, Research and Religions, Greece; National Research, Development and Innovation Office, Hungary; Department of Atomic Energy Government of India (DAE), Department of Science and Technology, Government of India (DST), University Grants Commission, Government of India (UGC), and Council of Scientific and Industrial Research (CSIR), India; Indonesian Institute of Science, Indonesia; Istituto Nazionale di Fisica Nucleare (INFN), Italy; Institute for Innovative Science and Technology, Nagasaki Institute of Applied Science (IIST), Japanese Ministry of Education, Culture, Sports, Science and Technology (MEXT), and Japan Society for the Promotion of Science (JSPS) KAKENHI, Japan; Consejo Nacional de Ciencia (CONACYT) y Tecnología, through Fondo de Cooperación Internacional en Ciencia y Tecnología (FONCICYT) and Dirección General de Asuntos del Personal Académico (DGAPA), Mexico; Nederlandse Organisatie voor Wetenschappelijk Onderzoek (NWO), Netherlands; the Research Council of Norway, Norway; Commission on Science and Technology for Sustainable

Development in the South (COMSATS), Pakistan; Pontificia Universidad Católica del Perú, Peru; Ministry of Education and Science, National Science Centre, and Warsaw University of Technology ID-UB Project Excellence Initiative, Poland; Korea Institute of Science and Technology Information and National Research Foundation of Korea (NRF), Republic of Korea; Ministry of Education and Scientific Research, Institute of Atomic Physics, and Ministry of Research and Innovation, and Institute of Atomic Physics, Romania; Joint Institute for Nuclear Research (JINR), Ministry of Education and Science of the Russian Federation, National Research Centre Kurchatov Institute, Russian Science Foundation, and Russian Foundation for Basic Research, Russia; Ministry of Education, Science, Research and Sport of the Slovak Republic, Slovakia; National Research Foundation of South Africa, South Africa; Swedish Research Council (VR) and Knut and Alice Wallenberg Foundation (KAW), Sweden; European Organization for Nuclear Research, Switzerland; Suranaree University of Technology (SUT), National Science and Technology Development Agency (NSDTA), and Office of the Higher Education Commission under NRU project of Thailand, Thailand; Turkish Energy, Nuclear and Mineral Research Agency (TENMAK), Turkey; National Academy of Sciences of Ukraine, Ukraine; Science and Technology Facilities Council (STFC), United Kingdom; National Science Foundation of the USA. (NSF) and U.S. Department of Energy, Office of Nuclear Physics (DOE NP), USA.

-
- [1] S. Acharya *et al.* (ALICE Collaboration), Λ_c^+ production in pp collisions at $\sqrt{s} = 7$ TeV and in p -Pb collisions at $\sqrt{s_{NN}} = 5.02$ TeV, *J. High Energy Phys.* **04** (2018) 108.
 - [2] S. Acharya *et al.* (ALICE Collaboration), First measurement of Ξ_c^0 production in pp collisions at $\sqrt{s} = 7$ TeV, *Phys. Lett. B* **781**, 8 (2018).
 - [3] S. Acharya *et al.* (ALICE Collaboration), Λ_c^+ Production and Baryon-to-Meson Ratios in pp and p -Pb Collisions at $\sqrt{s_{NN}} = 5.02$ TeV at the LHC, *Phys. Rev. Lett.* **127**, 202301 (2021).
 - [4] S. Acharya *et al.* (ALICE Collaboration), Λ_c^+ production in pp and in p -Pb collisions at $\sqrt{s_{NN}} = 5.02$ TeV, *Phys. Rev. C* **104**, 054905 (2021).
 - [5] A. M. Sirunyan *et al.* (CMS Collaboration), Production of Λ_c^+ baryons in proton-proton and lead-lead collisions at $\sqrt{s_{NN}} = 5.02$ TeV, *Phys. Lett. B* **803**, 135328 (2020).
 - [6] R. Aaij *et al.* (LHCb Collaboration), Prompt charm production in pp collisions at $\sqrt{s} = 7$ TeV, *Nucl. Phys.* **B871**, 1 (2013).
 - [7] R. Aaij *et al.* (LHCb Collaboration), Study of the production of Λ_b^0 and \bar{B}^0 hadrons in pp collisions and first measurement of the $\Lambda_b^0 \rightarrow J/\psi p K^-$ branching fraction, *Chin. Phys. C* **40**, 011001 (2016).

- [8] R. Aaij *et al.* (LHCb Collaboration), Measurement of b hadron fractions in 13 TeV pp collisions, *Phys. Rev. D* **100**, 031102 (2019).
- [9] R. Barate *et al.* (ALEPH Collaboration), Study of charm production in Z decays, *Eur. Phys. J. C* **16**, 597 (2000).
- [10] G. Alexander *et al.* (OPAL Collaboration), A study of charm hadron production in $Z^0 \rightarrow c\bar{c}$ and $Z^0 \rightarrow b\bar{b}$ decays at LEP, *Z. Phys. C* **72**, 1 (1996).
- [11] P. Abreu *et al.* (DELPHI Collaboration), Measurements of the Z partial decay width into $c\bar{c}$ and multiplicity of charm quarks per b decay, *Eur. Phys. J. C* **12**, 225 (2000).
- [12] L. Gladilin, Fragmentation fractions of c and b quarks into charmed hadrons at LEP, *Eur. Phys. J. C* **75**, 19 (2015).
- [13] S. Chekanov *et al.* (ZEUS Collaboration), Measurement of charm fragmentation ratios and fractions in photoproduction at HERA, *Eur. Phys. J. C* **44**, 351 (2005).
- [14] H. Abramowicz *et al.* (ZEUS Collaboration), Measurement of D^+ and Λ_c^+ production in deep inelastic scattering at HERA, *J. High Energy Phys.* **11** (2010) 009.
- [15] H. Abramowicz *et al.* (ZEUS Collaboration), Measurement of charm fragmentation fractions in photoproduction at HERA, *J. High Energy Phys.* **09** (2013) 058.
- [16] M. Cacciari, M. Greco, and P. Nason, The p_T spectrum in heavy flavor hadroproduction, *J. High Energy Phys.* **05** (1998) 007.
- [17] M. Cacciari, S. Frixione, N. Houdeau, M. L. Mangano, P. Nason, and G. Ridolfi, Theoretical predictions for charm and bottom production at the LHC, *J. High Energy Phys.* **10** (2012) 137.
- [18] B. A. Kniehl, G. Kramer, I. Schienbein, and H. Spiesberger, Inclusive $D^{*\pm}$ production in p anti- p collisions with massive charm quarks, *Phys. Rev. D* **71**, 014018 (2005).
- [19] B. Kniehl, G. Kramer, I. Schienbein, and H. Spiesberger, Inclusive charmed-meson production at the CERN LHC, *Eur. Phys. J. C* **72**, 2082 (2012).
- [20] M. Benzke, M. Garzelli, B. Kniehl, G. Kramer, S. Moch, and G. Sigl, Prompt neutrinos from atmospheric charm in the general-mass variable-flavour-number scheme, *J. High Energy Phys.* **12** (2017) 021.
- [21] G. Kramer and H. Spiesberger, Study of heavy meson production in p -Pb collisions at $\sqrt{s} = 5.02$ TeV in the general-mass variable-flavour-number scheme, *Nucl. Phys.* **B925**, 415 (2017).
- [22] I. Helenius and H. Paukkunen, Revisiting the D -meson hadroproduction in general-mass variable flavour number scheme, *J. High Energy Phys.* **05** (2018) 196.
- [23] B. A. Kniehl, G. Kramer, I. Schienbein, and H. Spiesberger, Λ_c^\pm production in pp collisions with a new fragmentation function, *Phys. Rev. D* **101**, 114021 (2020).
- [24] M. Niiyama *et al.* (Belle Collaboration), Production cross sections of hyperons and charmed baryons from e^+e^- annihilation near $\sqrt{s} = 10.52$ GeV, *Phys. Rev. D* **97**, 072005 (2018).
- [25] J. R. Christiansen and P. Z. Skands, String formation beyond leading colour, *J. High Energy Phys.* **08** (2015) 003.
- [26] M. He and R. Rapp, Charm-baryon production in proton-proton collisions, *Phys. Lett. B* **795**, 117 (2019).
- [27] S. Plumari, V. Minissale, S. K. Das, G. Coci, and V. Greco, Charmed hadrons from coalescence plus fragmentation in relativistic nucleus-nucleus collisions at RHIC and LHC, *Eur. Phys. J. C* **78**, 348 (2018).
- [28] V. Minissale, S. Plumari, and V. Greco, Charm hadrons in pp collisions at LHC energy within a coalescence plus fragmentation approach, *Phys. Lett. B* **821**, 136622 (2021).
- [29] J. Song, H.-h. Li, and F.-l. Shao, New feature of low p_T charm quark hadronization in pp collisions at $\sqrt{s} = 7$ TeV, *Eur. Phys. J. C* **78**, 344 (2018).
- [30] D. Ebert, R. N. Faustov, and V. O. Galkin, Spectroscopy and Regge trajectories of heavy baryons in the relativistic quark-diquark picture, *Phys. Rev. D* **84**, 014025 (2011).
- [31] A. Andronic, P. Braun-Munzinger, K. Redlich, and J. Stachel, Statistical hadronization of charm in heavy ion collisions at SPS, RHIC and LHC, *Phys. Lett. B* **571**, 36 (2003).
- [32] K. Aamodt *et al.* (ALICE Collaboration), The ALICE experiment at the CERN LHC, *J. Instrum.* **3**, S08002 (2008).
- [33] B. Abelev *et al.* (ALICE Collaboration), Performance of the ALICE experiment at the CERN LHC, *Int. J. Mod. Phys. A* **29**, 1430044 (2014).
- [34] J. Adam *et al.* (ALICE Collaboration), Determination of the event collision time with the ALICE detector at the LHC, *Eur. Phys. J. Plus* **132**, 99 (2017).
- [35] S. Acharya *et al.* (ALICE Collaboration), ALICE 2016-2017-2018 luminosity determination for pp collisions at $\sqrt{s} = 13$ TeV, Technical Report No. ALICE-PUBLIC-2021-005, CERN, 2021, <https://cds.cern.ch/record/2776672>.
- [36] P. Zyla *et al.* (Particle Data Group Collaboration), Review of particle physics, *Prog. Theor. Exp. Phys.* **2020**, 083C01 (2020).
- [37] S. Acharya *et al.* (ALICE Collaboration), Measurement of D^0 , D^+ , D^{*+} and D_s^+ production in pp collisions at $\sqrt{s} = 5.02$ TeV with ALICE, *Eur. Phys. J. C* **79**, 388 (2019).
- [38] J. Adam *et al.* (ALICE Collaboration), Particle identification in ALICE: a Bayesian approach, *Eur. Phys. J. Plus* **131**, 168 (2016).
- [39] A. Hoecker, P. Speckmayer, J. Stelzer, J. Therhaag, E. von Toerne, and H. Voss, TMVA: Toolkit for multivariate data analysis, *Proc. Sci.*, ACAT2007 (2007) 040 [arXiv:physics/0703039].
- [40] S. Acharya *et al.* (ALICE Collaboration), Measurement of D -meson production at mid-rapidity in pp collisions at $\sqrt{s} = 7$ TeV, *Eur. Phys. J. C* **77**, 550 (2017).
- [41] See Supplemental Material at <http://link.aps.org/supplemental/10.1103/PhysRevLett.128.012001> for more examples of the invariant-mass fits and the description of the background functions.
- [42] T. Sjöstrand, S. Mrenna, and P. Z. Skands, PYTHIA6.4 physics and manual, *J. High Energy Phys.* **05** (2006) 026.
- [43] T. Sjöstrand, S. Ask, J. R. Christiansen, R. Corke, N. Desai, P. Ilten, S. Mrenna, S. Prestel, C. O. Rasmussen, and P. Z. Skands, An introduction to PYTHIA8.2, *Comput. Phys. Commun.* **191**, 159 (2015).
- [44] R. Brun, F. Bruyant, F. Carminati, S. Giani, M. Maire, A. McPherson, G. Patrick, and L. Urban, GEANT: Detector

- description and simulation tool; Oct 1994. CERN Program Library, CERN, Geneva, 1993, <http://cds.cern.ch/record/1082634>.
- [45] T. Sjöstrand, S. Mrenna, and P.Z. Skands, A brief introduction to PYTHIA8.1, *Comput. Phys. Commun.* **178**, 852 (2008).
- [46] H. Albrecht *et al.* (ARGUS Collaboration), Observation of the charmed baryon $\Lambda(c)$ in e^+e^- annihilation at 10 GeV, *Phys. Lett. B* **207**, 109 (1988).
- [47] P. Avery *et al.* (CLEO Collaboration), Inclusive production of the charmed baryon Λ_c from e^+e^- annihilations at $\sqrt{s} = 10.55$ GeV, *Phys. Rev. D* **43**, 3599 (1991).
- [48] H. Albrecht *et al.* (ARGUS Collaboration), Inclusive production of D^0 , D^+ and D^{*+} (2010) mesons in B decays and nonresonant e^+e^- annihilation at 10.6 GeV, *Z. Phys. C* **52**, 353 (1991).

S. Acharya,¹⁴³ D. Adamová,⁹⁸ A. Adler,⁷⁶ J. Adolfsson,⁸³ G. Aglieri Rinella,³⁵ M. Agnello,³¹ N. Agrawal,⁵⁵ Z. Ahammed,¹⁴³ S. Ahmad,¹⁶ S. U. Ahn,⁷⁸ I. Ahuja,³⁹ Z. Akbar,⁵² A. Akindinov,⁹⁵ M. Al-Turany,¹¹⁰ S. N. Alam,⁴¹ D. Aleksandrov,⁹¹ B. Alessandro,⁶¹ H. M. Alfanda,⁷ R. Alfaro Molina,⁷³ B. Ali,¹⁶ Y. Ali,¹⁴ A. Alici,²⁶ N. Alizadehvandchali,¹²⁷ A. Alkin,³⁵ J. Alme,²¹ T. Alt,⁷⁰ L. Altenkamper,²¹ I. Altsybeev,¹¹⁵ M. N. Anaam,⁷ C. Andrei,⁴⁹ D. Andreou,⁹³ A. Andronic,¹⁴⁶ M. Angeletti,³⁵ V. Anguelov,¹⁰⁷ F. Antinori,⁵⁸ P. Antonioli,⁵⁵ C. Anuj,¹⁶ N. Apadula,⁸² L. Aphecetche,¹¹⁷ H. Appelshäuser,⁷⁰ S. Arcelli,²⁶ R. Arnaldi,⁶¹ I. C. Arsene,²⁰ M. Arslanok,^{107,148} A. Augustinus,³⁵ R. Averbeck,¹¹⁰ S. Aziz,⁸⁰ M. D. Azmi,¹⁶ A. Badalà,⁵⁷ Y. W. Baek,⁴² X. Bai,^{110,131} R. Bailhache,⁷⁰ Y. Bailung,⁵¹ R. Bala,¹⁰⁴ A. Balbino,³¹ A. Baldisseri,¹⁴⁰ B. Balis,² M. Ball,⁴⁴ D. Banerjee,⁴ R. Barbera,²⁷ L. Barioglio,^{25,108} M. Barlou,⁸⁷ G. G. Barnaföldi,¹⁴⁷ L. S. Barnby,⁹⁷ V. Barret,¹³⁷ C. Bartels,¹³⁰ K. Barth,³⁵ E. Bartsch,⁷⁰ F. Baruffaldi,²⁸ N. Bastid,¹³⁷ S. Basu,⁸³ G. Batigne,¹¹⁷ B. Batyunya,⁷⁷ D. Bauri,⁵⁰ J. L. Bazo Alba,¹¹⁴ I. G. Bearden,⁹² C. Beattie,¹⁴⁸ I. Belikov,¹³⁹ A. D. C. Bell Hechavarria,¹⁴⁶ F. Bellini,^{26,35} R. Bellwied,¹²⁷ S. Belokurova,¹¹⁵ V. Belyaev,⁹⁶ G. Bencedi,⁷¹ S. Beole,²⁵ A. Bercuci,⁴⁹ Y. Berdnikov,¹⁰¹ A. Berdnikova,¹⁰⁷ L. Bergmann,¹⁰⁷ M. G. Besoiu,⁶⁹ L. Betev,³⁵ P. P. Bhaduri,¹⁴³ A. Bhasin,¹⁰⁴ M. A. Bhat,⁴ B. Bhattacharjee,⁴³ P. Bhattacharya,²³ L. Bianchi,²⁵ N. Bianchi,⁵³ J. Bielčik,³⁸ J. Bielčíková,⁹⁸ J. Biernat,¹²⁰ A. Bilandzic,¹⁰⁸ G. Biro,¹⁴⁷ S. Biswas,⁴ J. T. Blair,¹²¹ D. Blau,⁹¹ M. B. Blidaru,¹¹⁰ C. Blume,⁷⁰ G. Boca,^{29,59} F. Bock,⁹⁹ A. Bogdanov,⁹⁶ S. Boi,²³ J. Bok,⁶³ L. Boldizsár,¹⁴⁷ A. Bolozdynya,⁹⁶ M. Bombara,³⁹ P. M. Bond,³⁵ G. Bonomi,^{59,142} H. Borel,¹⁴⁰ A. Borissov,⁸⁴ H. Bossi,¹⁴⁸ E. Botta,²⁵ L. Bratrud,⁷⁰ P. Braun-Munzinger,¹¹⁰ M. Bregant,¹²³ M. Broz,³⁸ G. E. Bruno,^{34,109} M. D. Buckland,¹³⁰ D. Budnikov,¹¹¹ H. Buesching,⁷⁰ S. Bufalino,³¹ O. Bugnon,¹¹⁷ P. Buhler,¹¹⁶ Z. Buthelezi,^{74,134} J. B. Butt,¹⁴ S. A. Bysiak,¹²⁰ D. Caffarri,⁹³ M. Cai,^{7,28} H. Caines,¹⁴⁸ A. Caliva,¹¹⁰ E. Calvo Villar,¹¹⁴ J. M. M. Camacho,¹²² R. S. Camacho,⁴⁶ P. Camerini,²⁴ F. D. M. Canedo,¹²³ F. Carnesecchi,^{26,35} R. Caron,¹⁴⁰ J. Castillo Castellanos,¹⁴⁰ E. A. R. Casula,²³ F. Catalano,³¹ C. Ceballos Sanchez,⁷⁷ P. Chakraborty,⁵⁰ S. Chandra,¹⁴³ S. Chapeland,³⁵ M. Chartier,¹³⁰ S. Chattopadhyay,¹⁴³ S. Chattopadhyay,¹¹² A. Chauvin,²³ T. G. Chavez,⁴⁶ C. Cheshkov,¹³⁸ B. Cheynis,¹³⁸ V. Chibante Barroso,³⁵ D. D. Chinellato,¹²⁴ S. Cho,⁶³ P. Chochula,³⁵ P. Christakoglou,⁹³ C. H. Christensen,⁹² P. Christiansen,⁸³ T. Chujo,¹³⁶ C. Cicalo,⁵⁶ L. Cifarelli,²⁶ F. Cindolo,⁵⁵ M. R. Ciupek,¹¹⁰ G. Clai,^{55,‡} J. Cleymans,^{126,†} F. Colamaria,⁵⁴ J. S. Colburn,¹¹³ D. Colella,^{34,54,109,147} A. Collu,⁸² M. Colocci,^{26,35} M. Concas,^{61,§} G. Conesa Balbastre,⁸¹ Z. Conesa del Valle,⁸⁰ G. Contin,²⁴ J. G. Contreras,³⁸ M. L. Coquet,¹⁴⁰ T. M. Cormier,⁹⁹ P. Cortese,³² M. R. Cosentino,¹²⁵ F. Costa,³⁵ S. Costanza,^{29,59} P. Crochet,¹³⁷ E. Cuautele,⁷¹ P. Cui,⁷ L. Cunqueiro,⁹⁹ A. Dainese,⁵⁸ F. P. A. Damas,^{117,140} M. C. Danisch,¹⁰⁷ A. Danu,⁶⁹ I. Das,¹¹² P. Das,⁸⁹ P. Das,⁴ S. Das,⁴ S. Dash,⁵⁰ S. De,⁸⁹ A. De Caro,³⁰ G. de Cataldo,⁵⁴ L. De Cilladi,²⁵ J. de Cuveland,⁴⁰ A. De Falco,²³ D. De Gruttola,³⁰ N. De Marco,⁶¹ C. De Martin,²⁴ S. De Pasquale,³⁰ S. Deb,⁵¹ H. F. Degenhardt,¹²³ K. R. Deja,¹⁴⁴ L. Dello Stritto,³⁰ S. Delsanto,²⁵ W. Deng,⁷ P. Dhankher,¹⁹ D. Di Bari,³⁴ A. Di Mauro,³⁵ R. A. Diaz,⁸ T. Dietel,¹²⁶ Y. Ding,^{7,138} R. Divià,³⁵ D. U. Dixit,¹⁹ Ø. Djuvsland,²¹ U. Dmitrieva,⁶⁵ J. Do,⁶³ A. Dobrin,⁶⁹ B. Dönigus,⁷⁰ O. Dordic,²⁰ A. K. Dubey,¹⁴³ A. Dubla,^{93,110} S. Dudi,¹⁰³ M. Dukhishyam,⁸⁹ P. Dupieux,¹³⁷ N. Dzalaiiova,¹³ T. M. Eder,¹⁴⁶ R. J. Ehlers,⁹⁹ V. N. Eikeland,²¹ F. Eisenhut,⁷⁰ D. Elia,⁵⁴ B. Erazmus,¹¹⁷ F. Ercolessi,²⁶ F. Erhardt,¹⁰² A. Erokhin,¹¹⁵ M. R. Erdsdal,²¹ B. Espagnon,⁸⁰ G. Eulisse,³⁵ D. Evans,¹¹³ S. Evdokimov,⁹⁴ L. Fabbietti,¹⁰⁸ M. Faggin,²⁸ J. Faivre,⁸¹ F. Fan,⁷ A. Fantoni,⁵³ M. Fasel,⁹⁹ P. Fecchio,³¹ A. Feliciello,⁶¹ G. Feofilov,¹¹⁵ A. Fernández Téllez,⁴⁶ A. Ferrero,¹⁴⁰ A. Ferretti,²⁵ V. J. G. Feuillard,¹⁰⁷ J. Figiel,¹²⁰ S. Filchagin,¹¹¹ D. Finogeev,⁶⁵ F. M. Fionda,^{21,56} G. Fiorenza,^{35,109} F. Flor,¹²⁷ A. N. Flores,¹²¹ S. Foertsch,⁷⁴ P. Foka,¹¹⁰ S. Fokin,⁹¹ E. Fragiaco,⁶² E. Frajna,¹⁴⁷ U. Fuchs,³⁵ N. Funicello,³⁰ C. Furget,⁸¹ A. Furs,⁶⁵ J. J. Gaardhøje,⁹² M. Gagliardi,²⁵ A. M. Gago,¹¹⁴ A. Gal,¹³⁹ C. D. Galvan,¹²² P. Ganoti,⁸⁷ C. Garabatos,¹¹⁰ J. R. A. Garcia,⁴⁶ E. Garcia-Solis,¹⁰ K. Garg,¹¹⁷ C. Gargiulo,³⁵ A. Garibli,⁹⁰

K. Garner,¹⁴⁶ P. Gasik,¹¹⁰ E. F. Gauger,¹²¹ A. Gautam,¹²⁹ M. B. Gay Ducati,⁷² M. Germain,¹¹⁷ P. Ghosh,¹⁴³ S. K. Ghosh,⁴ M. Giacalone,²⁶ P. Gianotti,⁵³ P. Giubellino,^{61,110} P. Giubilato,²⁸ A. M. C. Glaenger,¹⁴⁰ P. Glässel,¹⁰⁷ D. J. Q. Goh,⁸⁵ V. Gonzalez,¹⁴⁵ L. H. González-Trueba,⁷³ S. Gorbunov,⁴⁰ M. Gorgon,² L. Görlich,¹²⁰ S. Gotovac,³⁶ V. Grabski,⁷³ L. K. Graczykowski,¹⁴⁴ L. Greiner,⁸² A. Grelli,⁶⁴ C. Grigoras,³⁵ V. Grigoriev,⁹⁶ A. Grigoryan,^{1,†} S. Grigoryan,^{1,77} O. S. Groetvik,²¹ F. Grosa,^{35,61} J. F. Grosse-Oetringhaus,³⁵ R. Grosso,¹¹⁰ G. G. Guardiano,¹²⁴ R. Guernane,⁸¹ M. Guilbaud,¹¹⁷ K. Gulbrandsen,⁹² T. Gunji,¹³⁵ A. Gupta,¹⁰⁴ R. Gupta,¹⁰⁴ S. P. Guzman,⁴⁶ L. Gyulai,¹⁴⁷ M. K. Habib,¹¹⁰ C. Hadjidakis,⁸⁰ G. Halimoglu,⁷⁰ H. Hamagaki,⁸⁵ G. Hamar,¹⁴⁷ M. Hamid,⁷ R. Hannigan,¹²¹ M. R. Haque,^{89,144} A. Harlanderova,¹¹⁰ J. W. Harris,¹⁴⁸ A. Harton,¹⁰ J. A. Hasenbichler,³⁵ H. Hassan,⁹⁹ D. Hatzifotiadou,⁵⁵ P. Hauer,⁴⁴ L. B. Havener,¹⁴⁸ S. Hayashi,¹³⁵ S. T. Heckel,¹⁰⁸ E. Hellbär,⁷⁰ H. Helstrup,³⁷ T. Herman,³⁸ E. G. Hernandez,⁴⁶ G. Herrera Corral,⁹ F. Herrmann,¹⁴⁶ K. F. Hetland,³⁷ H. Hillemanns,³⁵ C. Hills,¹³⁰ B. Hippolyte,¹³⁹ B. Hofman,⁶⁴ B. Hohlweger,^{93,108} J. Honermann,¹⁴⁶ G. H. Hong,¹⁴⁹ D. Horak,³⁸ S. Hornung,¹¹⁰ A. Horzyk,² R. Hosokawa,¹⁵ P. Hristov,³⁵ C. Hughes,¹³³ P. Huhn,⁷⁰ T. J. Humanic,¹⁰⁰ H. Hushnud,¹¹² L. A. Husova,¹⁴⁶ A. Hutson,¹²⁷ D. Hutter,⁴⁰ J. P. Iddon,^{35,130} R. Ilkaev,¹¹¹ H. Ilyas,¹⁴ M. Inaba,¹³⁶ G. M. Innocenti,³⁵ M. Ippolitov,⁹¹ A. Isakov,^{38,98} M. S. Islam,¹¹² M. Ivanov,¹¹⁰ V. Ivanov,¹⁰¹ V. Izucheev,⁹⁴ M. Jablonski,² B. Jacak,⁸² N. Jacazio,³⁵ P. M. Jacobs,⁸² S. Jadlovská,¹¹⁹ J. Jadlovsky,¹¹⁹ S. Jaelani,⁶⁴ C. Jahnke,^{123,124} M. J. Jakubowska,¹⁴⁴ A. Jalotra,¹⁰⁴ M. A. Janik,¹⁴⁴ T. Janson,⁷⁶ M. Jercic,¹⁰² O. Jevons,¹¹³ F. Jonas,^{99,146} P. G. Jones,¹¹³ J. M. Jowett,^{35,110} J. Jung,⁷⁰ M. Jung,⁷⁰ A. Junique,³⁵ A. Jusko,¹¹³ J. Kaewjai,¹¹⁸ P. Kalinak,⁶⁶ A. Kalweit,³⁵ V. Kaplin,⁹⁶ S. Kar,⁷ A. Karasu Uysal,⁷⁹ D. Karatovic,¹⁰² O. Karavichev,⁶⁵ T. Karavicheva,⁶⁵ P. Karczmarczyk,¹⁴⁴ E. Karpechev,⁶⁵ A. Kazantsev,⁹¹ U. Kerschull,⁷⁶ R. Keidel,⁴⁸ D. L. D. Keijdener,⁶⁴ M. Keil,³⁵ B. Ketzer,⁴⁴ Z. Khabanova,⁹³ A. M. Khan,⁷ S. Khan,¹⁶ A. Khanzadeev,¹⁰¹ Y. Kharlov,⁹⁴ A. Khatun,¹⁶ A. Khuntia,¹²⁰ B. Kileng,³⁷ B. Kim,^{17,63} C. Kim,¹⁷ D. Kim,¹⁴⁹ D. J. Kim,¹²⁸ E. J. Kim,⁷⁵ J. Kim,¹⁴⁹ J. S. Kim,⁴² J. Kim,¹⁰⁷ J. Kim,¹⁴⁹ J. Kim,⁷⁵ M. Kim,¹⁰⁷ S. Kim,¹⁸ T. Kim,¹⁴⁹ S. Kirsch,⁷⁰ I. Kisel,⁴⁰ S. Kiselev,⁹⁵ A. Kisiel,¹⁴⁴ J. P. Kitowski,² J. L. Klay,⁶ J. Klein,³⁵ S. Klein,⁸² C. Klein-Bösing,¹⁴⁶ M. Kleiner,⁷⁰ T. Klemenz,¹⁰⁸ A. Kluge,³⁵ A. G. Knospe,¹²⁷ C. Kobdaj,¹¹⁸ M. K. Köhler,¹⁰⁷ T. Kollegger,¹¹⁰ A. Kondratyev,⁷⁷ N. Kondratyeva,⁹⁶ E. Kondratyuk,⁹⁴ J. König,⁷⁰ S. A. Königstorfer,¹⁰⁸ P. J. Konopka,^{2,35} G. Kornakov,¹⁴⁴ S. D. Koryciak,² L. Koska,¹¹⁹ A. Kotliarov,⁹⁸ O. Kovalenko,⁸⁸ V. Kovalenko,¹¹⁵ M. Kowalski,¹²⁰ I. Králik,⁶⁶ A. Kravčáková,³⁹ L. Kreis,¹¹⁰ M. Krivda,^{66,113} F. Krizek,⁹⁸ K. Krizkova Gajdosova,³⁸ M. Kroesen,¹⁰⁷ M. Krüger,⁷⁰ E. Kryshen,¹⁰¹ M. Krzewicki,⁴⁰ V. Kučera,³⁵ C. Kuhn,¹³⁹ P. G. Kuijer,⁹³ T. Kumaoka,¹³⁶ D. Kumar,¹⁴³ L. Kumar,¹⁰³ N. Kumar,¹⁰³ S. Kundu,^{35,89} P. Kurashvili,⁸⁸ A. Kurepin,⁶⁵ A. B. Kurepin,⁶⁵ A. Kuryakin,¹¹¹ S. Kushpil,⁹⁸ J. Kvapil,¹¹³ M. J. Kweon,⁶³ J. Y. Kwon,⁶³ Y. Kwon,¹⁴⁹ S. L. La Pointe,⁴⁰ P. La Rocca,²⁷ Y. S. Lai,⁸² A. Lakrathok,¹¹⁸ M. Lamanna,³⁵ R. Langoy,¹³² K. Lapidus,³⁵ P. Larionov,⁵³ E. Laudi,³⁵ L. Lautner,^{35,108} R. Lavicka,³⁸ T. Lazareva,¹¹⁵ R. Lea,^{24,59,142} J. Lehrbach,⁴⁰ R. C. Lemmon,⁹⁷ I. León Monzón,¹²² E. D. Lesser,¹⁹ M. Lettrich,^{35,108} P. Lévai,¹⁴⁷ X. Li,¹¹ X. L. Li,⁷ J. Lien,¹³² R. Lietava,¹¹³ B. Lim,¹⁷ S. H. Lim,¹⁷ V. Lindenstruth,⁴⁰ A. Lindner,⁴⁹ C. Lippmann,¹¹⁰ A. Liu,¹⁹ J. Liu,¹³⁰ I. M. Lofnes,²¹ V. Loginov,⁹⁶ C. Loizides,⁹⁹ P. Loncar,³⁶ J. A. Lopez,¹⁰⁷ X. Lopez,¹³⁷ E. López Torres,⁸ J. R. Luhder,¹⁴⁶ M. Lunardon,²⁸ G. Luparello,⁶² Y. G. Ma,⁴¹ A. Maevskaya,⁶⁵ M. Mager,³⁵ T. Mahmoud,⁴⁴ A. Maire,¹³⁹ M. Malaev,¹⁰¹ N. M. Malik,¹⁰⁴ Q. W. Malik,²⁰ L. Malinina,^{77,||} D. Mal'Kevich,⁹⁵ N. Mallick,⁵¹ P. Malzacher,¹¹⁰ G. Mandaglio,^{33,57} V. Manko,⁹¹ F. Manso,¹³⁷ V. Manzari,⁵⁴ Y. Mao,⁷ J. Mareš,⁶⁸ G. V. Margagliotti,²⁴ A. Margotti,⁵⁵ A. Marín,¹¹⁰ C. Markert,¹²¹ M. Marquard,⁷⁰ N. A. Martin,¹⁰⁷ P. Martinengo,³⁵ J. L. Martinez,¹²⁷ M. I. Martínez,⁴⁶ G. Martínez García,¹¹⁷ S. Masciocchi,¹¹⁰ M. Maserà,²⁵ A. Masoni,⁵⁶ L. Massacrier,⁸⁰ A. Mastroserio,^{54,141} A. M. Mathis,¹⁰⁸ O. Matonoha,⁸³ P. F. T. Matuoka,¹²³ A. Matyja,¹²⁰ C. Mayer,¹²⁰ A. L. Mazuecos,³⁵ F. Mazzaschi,²⁵ M. Mazzilli,³⁵ M. A. Mazzoni,⁶⁰ J. E. Mdhului,¹³⁴ A. F. Mechler,⁷⁰ F. Meddi,²² Y. Melikyan,⁶⁵ A. Menchaca-Rocha,⁷³ E. Meninno,^{30,116} A. S. Menon,¹²⁷ M. Meres,¹³ S. Mhlanga,^{74,126} Y. Miake,¹³⁶ L. Micheletti,^{25,61} L. C. Migliorin,¹³⁸ D. L. Mihaylov,¹⁰⁸ K. Mikhaylov,^{77,95} A. N. Mishra,¹⁴⁷ D. Miśkowiec,¹¹⁰ A. Modak,⁴ A. P. Mohanty,⁶⁴ B. Mohanty,⁸⁹ M. Mohisin Khan,¹⁶ Z. Moravcova,⁹² C. Mordasini,¹⁰⁸ D. A. Moreira De Godoy,¹⁴⁶ L. A. P. Moreno,⁴⁶ I. Morozov,⁶⁵ A. Morsch,³⁵ T. Mrnjavac,³⁵ V. Muccifora,⁵³ E. Mudnic,³⁶ D. Mühlheim,¹⁴⁶ S. Muhuri,¹⁴³ J. D. Mulligan,⁸² A. Mulliri,²³ M. G. Munhoz,¹²³ R. H. Munzer,⁷⁰ H. Murakami,¹³⁵ S. Murray,¹²⁶ L. Musa,³⁵ J. Musinsky,⁶⁶ J. W. Myrcha,¹⁴⁴ B. Naik,^{50,134} R. Nair,⁸⁸ B. K. Nandi,⁵⁰ R. Nania,⁵⁵ E. Nappi,⁵⁴ M. U. Naru,¹⁴ A. F. Nassirpour,⁸³ A. Nath,¹⁰⁷ C. Nattrass,¹³³ A. Neagu,²⁰ L. Nellen,⁷¹ S. V. Nesbo,³⁷ G. Neskovic,⁴⁰ D. Nesterov,¹¹⁵ B. S. Nielsen,⁹² S. Nikolaev,⁹¹ S. Nikulin,⁹¹ V. Nikulin,¹⁰¹ F. Noferini,⁵⁵ S. Noh,¹² P. Nomokonov,⁷⁷ J. Norman,¹³⁰ N. Novitzky,¹³⁶ P. Nowakowski,¹⁴⁴ A. Nyanin,⁹¹ J. Nystrand,²¹ M. Ogino,⁸⁵ A. Ohlson,⁸³ V. A. Okorokov,⁹⁶ J. Oleniacz,¹⁴⁴ A. C. Oliveira Da Silva,¹³³ M. H. Oliver,¹⁴⁸ A. Onnerstad,¹²⁸ C. Oppedisano,⁶¹ A. Ortiz Velasquez,⁷¹ T. Osako,⁴⁷ A. Oskarsson,⁸³ J. Otwinowski,¹²⁰ K. Oyama,⁸⁵ Y. Pachmayer,¹⁰⁷

S. Padhan,⁵⁰ D. Pagano,^{59,142} G. Paić,⁷¹ A. Palasciano,⁵⁴ J. Pan,¹⁴⁵ S. Panebianco,¹⁴⁰ P. Pareek,¹⁴³ J. Park,⁶³ J. E. Parkkila,¹²⁸
 S. P. Pathak,¹²⁷ R. N. Patra,^{35,104} B. Paul,²³ J. Pazzini,^{59,142} H. Pei,⁷ T. Peitzmann,⁶⁴ X. Peng,⁷ L. G. Pereira,⁷²
 H. Pereira Da Costa,¹⁴⁰ D. Peresunko,⁹¹ G. M. Perez,⁸ S. Perrin,¹⁴⁰ Y. Pestov,⁵ V. Petráček,³⁸ M. Petrovici,⁴⁹ R. P. Pezzi,^{72,117}
 S. Piano,⁶² M. Pikna,¹³ P. Pillot,¹¹⁷ O. Pinazza,^{35,55} L. Pinsky,¹²⁷ C. Pinto,²⁷ S. Pisano,⁵³ M. Płoskoń,⁸² M. Planinic,¹⁰²
 F. Pliquet,⁷⁰ M. G. Poghosyan,⁹⁹ B. Polichtchouk,⁹⁴ S. Politano,³¹ N. Poljak,¹⁰² A. Pop,⁴⁹ S. Porteboeuf-Houssais,¹³⁷
 J. Porter,⁸² V. Pozdniakov,⁷⁷ S. K. Prasad,⁴ R. Preghenella,⁵⁵ F. Prino,⁶¹ C. A. Pruneau,¹⁴⁵ I. Pshenichnov,⁶⁵ M. Puccio,³⁵
 S. Qiu,⁹³ L. Quaglia,²⁵ R. E. Quishpe,¹²⁷ S. Ragoni,¹¹³ A. Rakotozafindrabe,¹⁴⁰ L. Ramello,³² F. Rami,¹³⁹
 S. A. R. Ramirez,⁴⁶ A. G. T. Ramos,³⁴ T. A. Rancien,⁸¹ R. Raniwala,¹⁰⁵ S. Raniwala,¹⁰⁵ S. S. Räsänen,⁴⁵ R. Rath,⁵¹
 I. Ravasenga,⁹³ K. F. Read,^{99,133} A. R. Redelbach,⁴⁰ K. Redlich,^{88,¶} A. Rehman,²¹ P. Reichelt,⁷⁰ F. Reidt,³⁵
 H. A. Reme-ness,³⁷ R. Renfordt,⁷⁰ Z. Rescakova,³⁹ K. Reygers,¹⁰⁷ A. Riabov,¹⁰¹ V. Riabov,¹⁰¹ T. Richert,^{83,92} M. Richter,²⁰
 W. Riegler,³⁵ F. Riggi,²⁷ C. Ristea,⁶⁹ S. P. Rode,⁵¹ M. Rodríguez Cahuantzi,⁴⁶ K. Røed,²⁰ R. Rogalev,⁹⁴ E. Rogochaya,⁷⁷
 T. S. Rogoschinski,⁷⁰ D. Rohr,³⁵ D. Röhrich,²¹ P. F. Rojas,⁴⁶ P. S. Rokita,¹⁴⁴ F. Ronchetti,⁵³ A. Rosano,^{33,57} E. D. Rosas,⁷¹
 A. Rossi,⁵⁸ A. Rotondi,^{29,59} A. Roy,⁵¹ P. Roy,¹¹² S. Roy,⁵⁰ N. Rubini,²⁶ O. V. Rueda,⁸³ R. Rui,²⁴ B. Romyantsev,⁷⁷
 P. G. Russek,² A. Rustamov,⁹⁰ E. Ryabinkin,⁹¹ Y. Ryabov,¹⁰¹ A. Rybicki,¹²⁰ H. Rytkonen,¹²⁸ W. Rzesza,¹⁴⁴
 O. A. M. Saarimaki,⁴⁵ R. Sadek,¹¹⁷ S. Sadovsky,⁹⁴ J. Saetre,²¹ K. Šafařík,³⁸ S. K. Saha,¹⁴³ S. Saha,⁸⁹ B. Sahoo,⁵⁰ P. Sahoo,⁵⁰
 R. Sahoo,⁵¹ S. Sahoo,⁶⁷ D. Sahu,⁵¹ P. K. Sahu,⁶⁷ J. Saini,¹⁴³ S. Sakai,¹³⁶ S. Sambyal,¹⁰⁴ V. Samsonov,^{96,101,†} D. Sarkar,¹⁴⁵
 N. Sarkar,¹⁴³ P. Sarma,⁴³ V. M. Sarti,¹⁰⁸ M. H. P. Sas,¹⁴⁸ J. Schambach,^{99,121} H. S. Scheid,⁷⁰ C. Schiaua,⁴⁹ R. Schicker,¹⁰⁷
 A. Schmah,¹⁰⁷ C. Schmidt,¹¹⁰ H. R. Schmidt,¹⁰⁶ M. O. Schmidt,¹⁰⁷ M. Schmidt,¹⁰⁶ N. V. Schmidt,^{70,99} A. R. Schmier,¹³³
 R. Schotter,¹³⁹ J. Schukraft,³⁵ Y. Schutz,¹³⁹ K. Schwarz,¹¹⁰ K. Schweda,¹¹⁰ G. Scioli,²⁶ E. Scomparin,⁶¹ J. E. Seger,¹⁵
 Y. Sekiguchi,¹³⁵ D. Sekihata,¹³⁵ I. Selyuzhenkov,^{96,110} S. Senyukov,¹³⁹ J. J. Seo,⁶³ D. Serebryakov,⁶⁵ L. Šerkšnytė,¹⁰⁸
 A. Sevcenco,⁶⁹ T. J. Shaba,⁷⁴ A. Shabanov,⁶⁵ A. Shabetai,¹¹⁷ R. Shahoyan,³⁵ W. Shaikh,¹¹² A. Shangaraev,⁹⁴ A. Sharma,¹⁰³
 H. Sharma,¹²⁰ M. Sharma,¹⁰⁴ N. Sharma,¹⁰³ S. Sharma,¹⁰⁴ U. Sharma,¹⁰⁴ O. Sheibani,¹²⁷ K. Shigaki,⁴⁷ M. Shimomura,⁸⁶
 S. Shirinkin,⁹⁵ Q. Shou,⁴¹ Y. Sibiriak,⁹¹ S. Siddhanta,⁵⁶ T. Siemiarczuk,⁸⁸ T. F. Silva,¹²³ D. Silvermyr,⁸³ G. Simonetti,³⁵
 B. Singh,¹⁰⁸ R. Singh,⁸⁹ R. Singh,¹⁰⁴ R. Singh,⁵¹ V. K. Singh,¹⁴³ V. Singhal,¹⁴³ T. Sinha,¹¹² B. Sitar,¹³ M. Sitta,³²
 T. B. Skaali,²⁰ G. Skorodumovs,¹⁰⁷ M. Slupecki,⁴⁵ N. Smirnov,¹⁴⁸ R. J. M. Snellings,⁶⁴ C. Soncco,¹¹⁴ J. Song,¹²⁷
 A. Songmoolnak,¹¹⁸ F. Soramel,²⁸ S. Sorensen,¹³³ I. Sputowska,¹²⁰ J. Stachel,¹⁰⁷ I. Stan,⁶⁹ P. J. Steffanic,¹³³
 S. F. Stiefelmaier,¹⁰⁷ D. Stocco,¹¹⁷ I. Storehaug,²⁰ M. M. Storetvedt,³⁷ C. P. Stylianidis,⁹³ A. A. P. Suaide,¹²³ T. Sugitate,⁴⁷
 C. Suire,⁸⁰ M. Suljic,³⁵ R. Sultanov,⁹⁵ M. Šumbera,⁹⁸ V. Sumberia,¹⁰⁴ S. Sumowidagdo,⁵² S. Swain,⁶⁷ A. Szabo,¹³
 I. Szarka,¹³ U. Tabassam,¹⁴ S. F. Taghavi,¹⁰⁸ G. Taillepiéd,¹³⁷ J. Takahashi,¹²⁴ G. J. Tambave,²¹ S. Tang,^{7,137} Z. Tang,¹³¹
 M. Tarhini,¹¹⁷ M. G. Tazila,⁴⁹ A. Tauro,³⁵ G. Tejada Muñoz,⁴⁶ A. Telesca,³⁵ L. Terlizzi,²⁵ C. Terrevoli,¹²⁷ G. Tersimonov,³
 S. Thakur,¹⁴³ D. Thomas,¹²¹ R. Tieulent,¹³⁸ A. Tikhonov,⁶⁵ A. R. Timmins,¹²⁷ M. Tkacik,¹¹⁹ A. Toia,⁷⁰ N. Topilskaya,⁶⁵
 M. Toppi,⁵³ F. Torales-Acosta,¹⁹ T. Tork,⁸⁰ R. Cruz-Torres,⁸² S. R. Torres,³⁸ A. Trifiró,^{33,57} S. Tripathy,^{55,71} T. Tripathy,⁵⁰
 S. Trogolo,^{28,35} G. Trombetta,³⁴ V. Trubnikov,³ W. H. Trzaska,¹²⁸ T. P. Trzcinski,¹⁴⁴ B. A. Trzeciak,³⁸ A. Tumkin,¹¹¹
 R. Turrisi,⁵⁸ T. S. Tveter,²⁰ K. Ullaland,²¹ A. Uras,¹³⁸ M. Urioni,^{59,142} G. L. Usai,²³ M. Vala,³⁹ N. Valle,^{29,59} S. Vallerio,⁶¹
 N. van der Kolk,⁶⁴ L. V. R. van Doremalen,⁶⁴ M. van Leeuwen,⁹³ P. Vande Vyvre,³⁵ D. Varga,¹⁴⁷ Z. Varga,¹⁴⁷
 M. Varga-Kofarago,¹⁴⁷ A. Vargas,⁴⁶ M. Vasileiou,⁸⁷ A. Vasiliev,⁹¹ O. Vázquez Doce,¹⁰⁸ V. Vechernin,¹¹⁵ E. Vercellin,²⁵
 S. Vergara Limón,⁴⁶ L. Vermunt,⁶⁴ R. Vértesi,¹⁴⁷ M. Verweij,⁶⁴ L. Vickovic,³⁶ Z. Vilakazi,¹³⁴ O. Villalobos Baillie,¹¹³
 G. Vino,⁵⁴ A. Vinogradov,⁹¹ T. Virgili,³⁰ V. Vislavicius,⁹² A. Vodopyanov,⁷⁷ B. Volkel,³⁵ M. A. Völkl,¹⁰⁷ K. Voloshin,⁹⁵
 S. A. Voloshin,¹⁴⁵ G. Volpe,³⁴ B. von Haller,³⁵ I. Vorobyev,¹⁰⁸ D. Voscek,¹¹⁹ N. Vozniuk,⁶⁵ J. Vrláková,³⁹ B. Wagner,²¹
 C. Wang,⁴¹ D. Wang,⁴¹ M. Weber,¹¹⁶ R. J. G. V. Weelden,⁹³ A. Wegrzynek,³⁵ S. C. Wenzel,³⁵ J. P. Wessels,¹⁴⁶ J. Wiechula,⁷⁰
 J. Wikne,²⁰ G. Wilk,⁸⁸ J. Wilkinson,¹¹⁰ G. A. Willems,¹⁴⁶ B. Windelband,¹⁰⁷ M. Winn,¹⁴⁰ W. E. Witt,¹³³ J. R. Wright,¹²¹
 W. Wu,⁴¹ Y. Wu,¹³¹ R. Xu,⁷ S. Yalcin,⁷⁹ Y. Yamaguchi,⁴⁷ K. Yamakawa,⁴⁷ S. Yang,²¹ S. Yano,⁴⁷ Z. Yin,⁷ H. Yokoyama,⁶⁴
 I.-K. Yoo,¹⁷ J. H. Yoon,⁶³ S. Yuan,²¹ A. Yuncu,¹⁰⁷ V. Zaccolo,²⁴ A. Zaman,¹⁴ C. Zampolli,³⁵ H. J. C. Zanoli,⁶⁴ N. Zardoshti,³⁵
 A. Zarochentsev,¹¹⁵ P. Závada,⁶⁸ N. Zaviyalov,¹¹¹ H. Zbroszczyk,¹⁴⁴ M. Zhalov,¹⁰¹ S. Zhang,⁴¹ X. Zhang,⁷ Y. Zhang,¹³¹
 V. Zherebchevskii,¹¹⁵ Y. Zhi,¹¹ N. Zhigareva,⁹⁵ D. Zhou,⁷ Y. Zhou,⁹² J. Zhu,^{7,110} Y. Zhu,⁷ A. Zichichi,²⁶
 G. Zinovjev,³ and N. Zurlo^{59,142}

(ALICE Collaboration)

- ¹A. I. Alikhanyan National Science Laboratory (Yerevan Physics Institute) Foundation, Yerevan, Armenia
²AGH University of Science and Technology, Cracow, Poland
³Bogolyubov Institute for Theoretical Physics, National Academy of Sciences of Ukraine, Kiev, Ukraine
⁴Bose Institute, Department of Physics and Centre for Astroparticle Physics and Space Science (CAPSS), Kolkata, India
⁵Budker Institute for Nuclear Physics, Novosibirsk, Russia
⁶California Polytechnic State University, San Luis Obispo, California, USA
⁷Central China Normal University, Wuhan, China
⁸Centro de Aplicaciones Tecnológicas y Desarrollo Nuclear (CEADEN), Havana, Cuba
⁹Centro de Investigación y de Estudios Avanzados (CINVESTAV), Mexico City and Mérida, Mexico
¹⁰Chicago State University, Chicago, Illinois, USA
¹¹China Institute of Atomic Energy, Beijing, China
¹²Chungbuk National University, Cheongju, Republic of Korea
¹³Comenius University Bratislava, Faculty of Mathematics, Physics and Informatics, Bratislava, Slovakia
¹⁴COMSATS University Islamabad, Islamabad, Pakistan
¹⁵Creighton University, Omaha, Nebraska, USA
¹⁶Department of Physics, Aligarh Muslim University, Aligarh, India
¹⁷Department of Physics, Pusan National University, Pusan, Republic of Korea
¹⁸Department of Physics, Sejong University, Seoul, Republic of Korea
¹⁹Department of Physics, University of California, Berkeley, California, USA
²⁰Department of Physics, University of Oslo, Oslo, Norway
²¹Department of Physics and Technology, University of Bergen, Bergen, Norway
²²Dipartimento di Fisica dell'Università "La Sapienza" and Sezione INFN, Rome, Italy
²³Dipartimento di Fisica dell'Università and Sezione INFN, Cagliari, Italy
²⁴Dipartimento di Fisica dell'Università and Sezione INFN, Trieste, Italy
²⁵Dipartimento di Fisica dell'Università and Sezione INFN, Turin, Italy
²⁶Dipartimento di Fisica e Astronomia dell'Università and Sezione INFN, Bologna, Italy
²⁷Dipartimento di Fisica e Astronomia dell'Università and Sezione INFN, Catania, Italy
²⁸Dipartimento di Fisica e Astronomia dell'Università and Sezione INFN, Padova, Italy
²⁹Dipartimento di Fisica e Nucleare e Teorica, Università di Pavia, Pavia, Italy
³⁰Dipartimento di Fisica "E. R. Caianiello" dell'Università and Gruppo Collegato INFN, Salerno, Italy
³¹Dipartimento DISAT del Politecnico and Sezione INFN, Turin, Italy
³²Dipartimento di Scienze e Innovazione Tecnologica dell'Università del Piemonte Orientale and INFN Sezione di Torino, Alessandria, Italy
³³Dipartimento di Scienze MIFT, Università di Messina, Messina, Italy
³⁴Dipartimento Interateneo di Fisica "M. Merlin" and Sezione INFN, Bari, Italy
³⁵European Organization for Nuclear Research (CERN), Geneva, Switzerland
³⁶Faculty of Electrical Engineering, Mechanical Engineering and Naval Architecture, University of Split, Split, Croatia
³⁷Faculty of Engineering and Science, Western Norway University of Applied Sciences, Bergen, Norway
³⁸Faculty of Nuclear Sciences and Physical Engineering, Czech Technical University in Prague, Prague, Czech Republic
³⁹Faculty of Science, P.J. Šafárik University, Košice, Slovakia
⁴⁰Frankfurt Institute for Advanced Studies, Johann Wolfgang Goethe-Universität Frankfurt, Frankfurt, Germany
⁴¹Fudan University, Shanghai, China
⁴²Gangneung-Wonju National University, Gangneung, Republic of Korea
⁴³Gauhati University, Department of Physics, Guwahati, India
⁴⁴Helmholtz-Institut für Strahlen- und Kernphysik, Rheinische Friedrich-Wilhelms-Universität Bonn, Bonn, Germany
⁴⁵Helsinki Institute of Physics (HIP), Helsinki, Finland
⁴⁶High Energy Physics Group, Universidad Autónoma de Puebla, Puebla, Mexico
⁴⁷Hiroshima University, Hiroshima, Japan
⁴⁸Hochschule Worms, Zentrum für Technologietransfer und Telekommunikation (ZTT), Worms, Germany
⁴⁹Horia Hulubei National Institute of Physics and Nuclear Engineering, Bucharest, Romania
⁵⁰Indian Institute of Technology Bombay (IIT), Mumbai, India
⁵¹Indian Institute of Technology Indore, Indore, India
⁵²Indonesian Institute of Sciences, Jakarta, Indonesia
⁵³INFN, Laboratori Nazionali di Frascati, Frascati, Italy
⁵⁴INFN, Sezione di Bari, Bari, Italy
⁵⁵INFN, Sezione di Bologna, Bologna, Italy
⁵⁶INFN, Sezione di Cagliari, Cagliari, Italy
⁵⁷INFN, Sezione di Catania, Catania, Italy
⁵⁸INFN, Sezione di Padova, Padova, Italy

- ⁵⁹*INFN, Sezione di Pavia, Pavia, Italy*
⁶⁰*INFN, Sezione di Roma, Rome, Italy*
⁶¹*INFN, Sezione di Torino, Turin, Italy*
⁶²*INFN, Sezione di Trieste, Trieste, Italy*
⁶³*Inha University, Incheon, Republic of Korea*
⁶⁴*Institute for Gravitational and Subatomic Physics (GRASP), Utrecht University/Nikhef, Utrecht, Netherlands*
⁶⁵*Institute for Nuclear Research, Academy of Sciences, Moscow, Russia*
⁶⁶*Institute of Experimental Physics, Slovak Academy of Sciences, Košice, Slovakia*
⁶⁷*Institute of Physics, Homi Bhabha National Institute, Bhubaneswar, India*
⁶⁸*Institute of Physics of the Czech Academy of Sciences, Prague, Czech Republic*
⁶⁹*Institute of Space Science (ISS), Bucharest, Romania*
⁷⁰*Institut für Kernphysik, Johann Wolfgang Goethe-Universität Frankfurt, Frankfurt, Germany*
⁷¹*Instituto de Ciencias Nucleares, Universidad Nacional Autónoma de México, Mexico City, Mexico*
⁷²*Instituto de Física, Universidade Federal do Rio Grande do Sul (UFRGS), Porto Alegre, Brazil*
⁷³*Instituto de Física, Universidad Nacional Autónoma de México, Mexico City, Mexico*
⁷⁴*iThemba LABS, National Research Foundation, Somerset West, South Africa*
⁷⁵*Jeonbuk National University, Jeonju, Republic of Korea*
⁷⁶*Johann-Wolfgang-Goethe Universität Frankfurt Institut für Informatik, Fachbereich Informatik und Mathematik, Frankfurt, Germany*
⁷⁷*Joint Institute for Nuclear Research (JINR), Dubna, Russia*
⁷⁸*Korea Institute of Science and Technology Information, Daejeon, Republic of Korea*
⁷⁹*KTO Karatay University, Konya, Turkey*
⁸⁰*Laboratoire de Physique des 2 Infinis, Irène Joliot-Curie, Orsay, France*
⁸¹*Laboratoire de Physique Subatomique et de Cosmologie, Université Grenoble-Alpes, CNRS-IN2P3, Grenoble, France*
⁸²*Lawrence Berkeley National Laboratory, Berkeley, California, USA*
⁸³*Lund University Department of Physics, Division of Particle Physics, Lund, Sweden*
⁸⁴*Moscow Institute for Physics and Technology, Moscow, Russia*
⁸⁵*Nagasaki Institute of Applied Science, Nagasaki, Japan*
⁸⁶*Nara Women's University (NWU), Nara, Japan*
⁸⁷*National and Kapodistrian University of Athens, School of Science, Department of Physics, Athens, Greece*
⁸⁸*National Centre for Nuclear Research, Warsaw, Poland*
⁸⁹*National Institute of Science Education and Research, Homi Bhabha National Institute, Jatni, India*
⁹⁰*National Nuclear Research Center, Baku, Azerbaijan*
⁹¹*National Research Centre Kurchatov Institute, Moscow, Russia*
⁹²*Niels Bohr Institute, University of Copenhagen, Copenhagen, Denmark*
⁹³*Nikhef, National institute for subatomic physics, Amsterdam, Netherlands*
⁹⁴*NRC Kurchatov Institute IHEP, Protvino, Russia*
⁹⁵*NRC Kurchatov Institute—ITEP, Moscow, Russia*
⁹⁶*NRNU Moscow Engineering Physics Institute, Moscow, Russia*
⁹⁷*Nuclear Physics Group, STFC Daresbury Laboratory, Daresbury, United Kingdom*
⁹⁸*Nuclear Physics Institute of the Czech Academy of Sciences, Řež u Prahy, Czech Republic*
⁹⁹*Oak Ridge National Laboratory, Oak Ridge, Tennessee, USA*
¹⁰⁰*Ohio State University, Columbus, Ohio, USA*
¹⁰¹*Petersburg Nuclear Physics Institute, Gatchina, Russia*
¹⁰²*Physics department, Faculty of science, University of Zagreb, Zagreb, Croatia*
¹⁰³*Physics Department, Panjab University, Chandigarh, India*
¹⁰⁴*Physics Department, University of Jammu, Jammu, India*
¹⁰⁵*Physics Department, University of Rajasthan, Jaipur, India*
¹⁰⁶*Physikalisches Institut, Eberhard-Karls-Universität Tübingen, Tübingen, Germany*
¹⁰⁷*Physikalisches Institut, Ruprecht-Karls-Universität Heidelberg, Heidelberg, Germany*
¹⁰⁸*Physik Department, Technische Universität München, Munich, Germany*
¹⁰⁹*Politecnico di Bari and Sezione INFN, Bari, Italy*
¹¹⁰*Research Division and ExtreMe Matter Institute EMMI, GSI Helmholtzzentrum für Schwerionenforschung GmbH, Darmstadt, Germany*
¹¹¹*Russian Federal Nuclear Center (VNIIEF), Sarov, Russia*
¹¹²*Saha Institute of Nuclear Physics, Homi Bhabha National Institute, Kolkata, India*
¹¹³*School of Physics and Astronomy, University of Birmingham, Birmingham, United Kingdom*
¹¹⁴*Sección Física, Departamento de Ciencias, Pontificia Universidad Católica del Perú, Lima, Peru*
¹¹⁵*St. Petersburg State University, St. Petersburg, Russia*
¹¹⁶*Stefan Meyer Institut für Subatomare Physik (SMI), Vienna, Austria*
¹¹⁷*SUBATECH, IMT Atlantique, Université de Nantes, CNRS-IN2P3, Nantes, France*

- ¹¹⁸*Suranaree University of Technology, Nakhon Ratchasima, Thailand*
¹¹⁹*Technical University of Košice, Košice, Slovakia*
¹²⁰*The Henryk Niewodniczanski Institute of Nuclear Physics, Polish Academy of Sciences, Cracow, Poland*
¹²¹*The University of Texas at Austin, Austin, Texas, USA*
¹²²*Universidad Autónoma de Sinaloa, Culiacán, Mexico*
¹²³*Universidade de São Paulo (USP), São Paulo, Brazil*
¹²⁴*Universidade Estadual de Campinas (UNICAMP), Campinas, Brazil*
¹²⁵*Universidade Federal do ABC, Santo Andre, Brazil*
¹²⁶*University of Cape Town, Cape Town, South Africa*
¹²⁷*University of Houston, Houston, Texas, USA*
¹²⁸*University of Jyväskylä, Jyväskylä, Finland*
¹²⁹*University of Kansas, Lawrence, Kansas, USA*
¹³⁰*University of Liverpool, Liverpool, United Kingdom*
¹³¹*University of Science and Technology of China, Hefei, China*
¹³²*University of South-Eastern Norway, Tonsberg, Norway*
¹³³*University of Tennessee, Knoxville, Tennessee, USA*
¹³⁴*University of the Witwatersrand, Johannesburg, South Africa*
¹³⁵*University of Tokyo, Tokyo, Japan*
¹³⁶*University of Tsukuba, Tsukuba, Japan*
¹³⁷*Université Clermont Auvergne, CNRS/IN2P3, LPC, Clermont-Ferrand, France*
¹³⁸*Université de Lyon, CNRS/IN2P3, Institut de Physique des 2 Infinis de Lyon, Lyon, France*
¹³⁹*Université de Strasbourg, CNRS, IPHC UMR 7178, F-67000 Strasbourg, France, Strasbourg, France*
¹⁴⁰*Université Paris-Saclay Centre d'Etudes de Saclay (CEA), IRFU, Département de Physique Nucléaire (DPhN), Saclay, France*
¹⁴¹*Università degli Studi di Foggia, Foggia, Italy*
¹⁴²*Università di Brescia, Brescia, Italy*
¹⁴³*Variable Energy Cyclotron Centre, Homi Bhabha National Institute, Kolkata, India*
¹⁴⁴*Warsaw University of Technology, Warsaw, Poland*
¹⁴⁵*Wayne State University, Detroit, Michigan, USA*
¹⁴⁶*Westfälische Wilhelms-Universität Münster, Institut für Kernphysik, Münster, Germany*
¹⁴⁷*Wigner Research Centre for Physics, Budapest, Hungary*
¹⁴⁸*Yale University, New Haven, Connecticut, USA*
¹⁴⁹*Yonsei University, Seoul, Republic of Korea*

[†]Deceased.

[‡]Also at Italian National Agency for New Technologies, Energy and Sustainable Economic Development (ENEA), Bologna, Italy.

[§]Also at Dipartimento DET del Politecnico di Torino, Turin, Italy.

^{||}Also at M. V. Lomonosov Moscow State University, D. V. Skobeltsyn Institute of Nuclear, Physics, Moscow, Russia.

[¶]Also at Institute of Theoretical Physics, University of Wrocław, Poland.